High Pressure Research
Vol. 30, No. 2, June 2010, 224–229

Taylor & Francis
Taylor & Francis Group

Effect of dilution on the spin pairing transition in rhombohedral carbonates

Barbara Lavina[a]*, Przemyslaw Dera[b], Robert T. Downs[c], Oliver Tschauner[a,d], Wenge Yang[e,f], Olga Shebanova[e] and Guoyin Shen[e]

[a]*High Pressure Science and Engineering Center and Department of Physics, University of Nevada, Las Vegas, NV 89154, USA;* [b]*GSECARS, University of Chicago, Building 434A, 9700 South Cass Ave, Argonne, IL 60439, USA;* [c]*Department of Geosciences, University of Arizona, Tucson, AZ 85721-0077, USA;* [d]*Division of Geology and Planetary Sciences, California Institute of Technology, Pasadena, CA 91125, USA;* [e]*HPCAT, Carnegie Institution of Washington, Building 434E, 9700 South Cass Avenue, Argonne, IL 60439, USA;* [f]*HPSynC, Carnegie Institution of Washington, Advanced Photon Source, 9700 South Cass Avenue, Argonne, IL 60439, USA*

(*Received 19 January 2010; final version received 12 April 2010*)

The compressibility of an iron-bearing magnesite ($Mg_{0.87}Fe^{2+}_{0.12}Ca_{0.01}$)$CO_3$ was determined by means of single crystal diffraction up to 64 GPa. Up to 49 GPa the pressure-evolution of the unit cell volume of the solid solution with 12% of Fe^{2+} can be described by a third-order Birch–Murnaghan equation of state with parameters $V_0 = 281.0(5)$ Å^3, $K_0 = 102.8(3)$ GPa, $K'_0 = 5.44$. The spin pairing of the Fe^{2+} d-electrons occurs between 49 and 52 GPa, as evidenced by a discontinuous volume change. The transition pressure is increased by about 5 GPa compared with the iron end-member; an effect consistent with a cooperative contribution of adjacent clusters to the spin transition. The trend is, however, opposite in the periclase–wüstite solid solution. Differences among the two structures, in particular in the Fe–Fe interactions, that might explain the different behavior are discussed.

Keywords: magnesite; siderite, spin transition; compressibility; single crystal diffraction

1. Introduction

The study of the high-pressure behavior of Fe-bearing carbonates is relevant to the deep Earth carbon cycle, and constitutes an interesting case study of the structural effect of the pressure-induced spin pairing of Fe^{2+} d-electrons on mantle minerals. Whether or not carbonates survive the subduction process and reach the deep mantle is still under debate. While magnesite, $MgCO_3$, is stable up to lower mantle pressure- and temperature-conditions [1], its stability in association with mantle minerals is controversial [2,3]. The discovery of carbonate inclusions in diamonds of deep mantle origin [4] suggests that carbonates do exist, at least under particular conditions, in the deep Earth. The occurrence of the spin pairing transition of Fe^{2+} in siderite (Sd) was discovered by

*Corresponding author. Email: lavina.b1@gmail.com

ISSN 0895-7959 print/ISSN 1477-2299 online

DOI: 10.1080/08957959.2010.485391
http://www.informaworld.com

means of X-ray emission spectroscopy [5], then modeled from first principles calculations [6], and further investigated by means of single crystal diffraction [7]. The spin pairing of the Fe d-electrons was predicted to have occurred in mantle minerals about 50 years ago [8] but was observed only recently [9]. The spin pairing has important consequences for the physical properties of the mantle minerals and for the Fe partitioning. Given the complexity of natural systems, it is necessary to understand thoroughly the effect of T, P, composition, and structure on the occurrence and width of the spin transition [10,11,12]. Rhombohedral carbonates are among the few minerals where the concentration of mixed valence substitutions is negligible. Because of the symmetry constraints the six metal–ligand bond distances of the Fe^{2+}coordination sphere are equal, with only trigonal distortion of the octahedra allowed. Some of the factors usually complicating the behavior of the electronic phase transition, such as mixed valence for Fe^{2+} and the presence of structural sites of different size and geometry are conveniently absent in carbonates. In this work we study the effect of the Fe^{2+} concentration on the transition pressure. The composition of the iron-bearing magnesite (Fe–Mgs) selected for this study was chosen to be close to plausible mantle carbonate composition.

2. Experimental

The specimen chosen for the experiment is an iron-bearing magnesite from Tyrol (Austria), and was obtained from the RRUFF Project collection (http://rruff.info/R050676). Microprobe data from the RRUFF database lead to the structural formula $(Mg_{0.87}Fe^{2+}_{0.12}Ca_{0.01})CO_3$. The high pressure experiment was performed with a four-pin diamond anvil cell (DAC) equipped with a pair of one-third carat standard cut diamonds with 0.3 mm culet size. A Re foil, used as gasket material, was indented to a thickness of 35 μm, then a 120 μm diameter hole was drilled. A cleavage rhombohedron about 7 μm thick and 15 μm across was positioned at the center of the culet; a ruby sphere and gold powder were placed nearby to evaluate the pressure. After collecting the data at ambient pressure with the sample in the unsealed DAC, the sample chamber was filled with Ne at 172 MPa using the GSECARS/COMPRES gas loading system. Data were collected at the Advanced Photon Source (APS), Sector 16 (HPCAT), at the 16BMD station. A monochromatic beam of 33 keV was focussed to a spot size of about $8 \times 15\,\mu m^2$. The diffraction patterns were collected in the omega-scan mode ($\pm 15°$) using a MAR345 IP detector. Data were collected at three χ angles ($\chi 1 = 0°$, $\chi 2 \approx 30°$ $\chi 3 \approx -30°$) randomly set at each pressure step. At each χ angle a different set of reflections was sampled, changing χ might result in slightly more scattered data but ensures better accuracy. Diffraction peaks are symmetric and sharp up to the highest pressure reached (Figure 1(a)). For the data processing, the software FIT2D [13], GSE_ADA, and RSV [14] were used. A data set of 31 compression points was collected in the range 0–64 GPa (Table 1). Pressure was calculated from the 300 K isotherm of gold [15]. An example of the distribution of peaks in reciprocal space and the orientation of the cell in the laboratory reference system is shown in Figure 1(b).

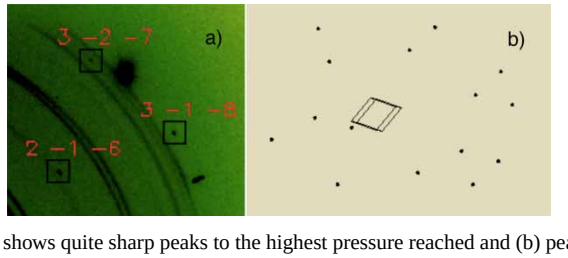

Figure 1. (a) The pattern shows quite sharp peaks to the highest pressure reached and (b) peaks in the reciprocal space are plot perpendicularly to the X-ray beam.

Table 1. Compressibility data of $(Mg_{0.87}Fe^{2+}_{0.12}Ca_{0.01})CO_3$.

P#	P (GPa)	a (Å)	c (Å)	V (Å^3)
RRUFF[a]	0.0001	4.64154(8)	15.0710(4)	281.19(1)
0_χ1[b]	0.0001	4.641(3)	15.07(2)	281.0(5)
1_χ1	0.45(4)	4.640(5)	15.05(2)	280.7(7)
2_χ1	7.25(3)	4.585(5)	14.58(2)	265.4(7)
3_χ1	9.95(10)	4.562(5)	14.45(2)	260.4(7)
4_χ2	13.93(4)	4.539(12)	14.25(6)	254(2)
5_χ2	19.91(4)	4.500(7)	13.98(3)	245.1(9)
5_χ1	21.11(3)	4.493(10)	13.95(7)	244(2)
6_χ1	26.30(10)	4.466(3)	13.79(2)	238.2(5)
6_χ2	26.21(10)	4.464(6)	13.79(3)	238.0(8)
7_χ1	32.84(8)	4.437(6)	13.61(3)	232.0(8)
8_χ1	36.05(10)	4.423(10)	13.53(4)	229.2(12)
8_χ2	36.38(10)	4.426(8)	13.50(4)	229.0(11)
9_χ2	38.8(10)	4.407(9)	13.50(4)	227.1(12)
10_χ1	39.82(5)	4.40695)	13.49(3)	226.8(7)
11_χ1	41.05(6)	4.402(5)	13.46(3)	225.9(7)
11_χ2	41.08(7)	4.399(7)	13.44(4)	225.3(10)
12_χ3	43.86(4)	4.388(5)	13.41(3)	223.6(7)
13_χ1	44.72(6)	4.390(5)	13.40(3)	223.6(7)
14_χ3	44.08(5)	4.384(4)	13.42(3)	223.4(6)
15_χ2	44.88(5)	4.380(8)	13.45(4)	223.4(11)
16_χ2	45.75(7)	4.375(4)	13.41(5)	222.2(9)
17_χ3	46.25(6)	4.381(4)	13.38(3)	222.4(6)
18_χ3	47.11(5)	4.369(5)	13.38(3)	221.1(7)
19_χ2	48.91(10)	4.369(6)	13.27(5)	219.4(10)
20_χ2	52.16(10)	4.349(6)	13.16(4)	215.6(9)
21_χ3	53.52(6)	4.34293)	13.18(3)	215.2(6)
22_χ2	55.12(10)	4.346(6)	13.08(3)	214.0(8)
23_χ3	56.32(8)	4.337(3)	13.05(3)	212.6(6)
24_χ2	56.85(10)	4.333(5)	13.06(3)	212.4(7)
25_χ3	62.8(10)	4.314(5)	12.96(6)	208.9(11)
26_χ2	64.81(9)	4.315(6)	12.94(4)	208.7(9)

Notes: [a]Value from the RRUFF database. [b]The notation χ1–3 refers to the χ angle at which the data were collected. Data were collected at three χ angles (χ1 = 0°, χ2 = 30° χ3 = −30°).

3. Results and discussion

In siderite containing 25% magnesite, the spin transition occurs at about 43 GPa with a concomitant volume decrease of 10% [7]. In Fe–Mgs, the small discontinuity in the compressibility (Figures 2 and 3) shows that the electronic transition occurs between 49 and 52 GPa. Change in color, very pronounced in siderite [7], was not observed in Fe–Mgs. It is likely that the lower Fe concentration and thinner crystal made the coloration less pronounced.

The compressibility of Fe–Mgs has been evaluated by fitting the K_0 parameter of the third-order Birch–Murnaghan equation of state (EOS) to the P–V data in the range 0–49 GPa [16]. K_0' was fixed to 5.44, the value recently proposed for pure magnesite [17]. The value obtained for K_0, 102.8(3) GPa, is slightly larger than the value for pure magnesite, 97.1(5) GPa [17], and in agreement with the increase in bulk modulus expected for the Fe concentration along the Mgs–Sd solid solution previously observed [18]. The axial compressibility, fitted with the same formalism but using the cubic power of the lattice parameters [16], and fixing K_0' to the values for magnesite [17] [$K_0'(a) = 8.3(4)$; $K_0'(c) = 3.6(1)$], is described by $K_0(a) = 131(1)$ GPa and $K_0(c) = 65.4(7)$ GPa. The large anisotropy of compression has clear structural reasons, as the small and rigid CO_3 units connected through faces of the octahedra are oriented perpendicular to the c-axis, with the compression along the a-axis hindered by the rigid C–O bonds and O–O

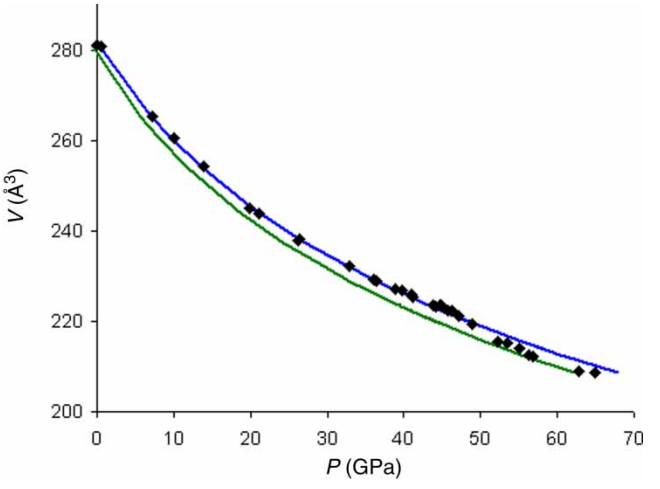

Figure 2. Volume compressibility of Fe–magnesite. The blue curve shows the third-order Birch Murnaghan EOS fitted to the data up to 49 GPa, and the green curve represents the pure magnesite EOS [17]. The size of the symbols roughly correspond to the error bar (color online).

repulsion. Conversely, no bond or edge is parallel to the *c* direction; as a result, the *c*-axis is three times more compressible than the *a*-axis. The volume of siderite in the low spin state is slightly smaller than the volume of magnesite at the same pressure [7]. After the spin transition the volume behavior of the Fe-magnesite is equal, within uncertainties, to that of magnesite (Figure 2).

The shift of the spin transition to higher pressure is opposite to the behavior observed for the periclase–wüstite solid solution [19]. There are important structural differences between the two minerals that might be responsible for their opposite behavior. A different pressure of the spin transition between the two minerals can be attributed to the different strength of the ligands (*cf.* the spectrochemical series), while the different behavior with dilution might be due to different Fe–Fe interactions and/or local strain induced by the size mismatch of neighboring clusters. While the first Fe^{2+} coordination sphere differs only slightly between the two structures, with a regular octahedron in the oxide and a slightly trigonally distorted octahedron in the carbonate, the Fe–Fe coordination sphere differs substantially. In ferropericlase, octahedra share all their 12 edges with their neighbors, resulting in a short distance between octahedral cations (about 3 Å at ambient pressure) which implies that even at relatively low Fe concentration there is a strong Fe–Fe interaction, which will increase with pressure. In the carbonate, adjacent octahedra share only their six corners, with a distance between octahedral cations of about 3.3 Å at ambient pressure. As a result, the Fe–Fe nearest-neighbor interaction is weaker in the carbonate than in ferropericlase. Furthermore, the number of interactions decreases twice as fast with Fe dilution compared with ferropericlase, where the transition pressure increases strongly with the Fe content. In the pure iron carbonate, first principle calculations show that after the spin transition the Fe–Fe interaction becomes a weak bonding [6]. If the Fe–Fe interaction contributes to the spin pairing transition either via bonding or strain, its effect would rapidly decrease with Fe dilution in the carbonate, then it is plausible that a greater pressure, further decreasing the Fe–O distance and increasing the spin pairing energy, might be required in a diluted Fe carbonate with respect to a concentrated one. Conceivably in ferropericlase the repulsion between adjacent HS–Fe^{2+} inhibits the spin pairing by imposing an anomalously large Fe–O bond length [20]. At ambient pressure the distance is 2.167 Å [21] and 2.144 Å in wüstite (extrapolated) and siderite, respectively. In the dilute sample instead, the Fe–Fe repulsion is decreased and, if the structure is not relaxed at the level of the first coordination sphere, the strain imposed by the small Mg cation reduces the local Fe–O bond length in ferropericlase, reducing the external pressure required for the spin pairing.

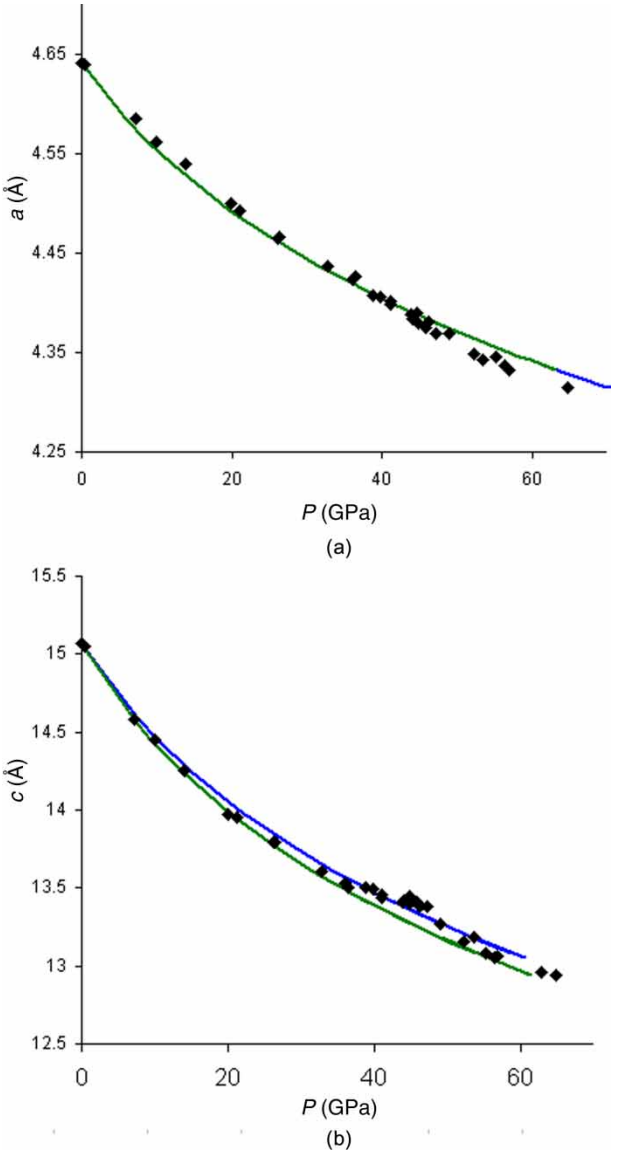

Figure 3. Linear compressibility of the cell parameters a (a) and c (b). The blue curves show the third-order Birch Murnaghan EOS fitted to the data up to 49 GPa, the green curves were calculated with the pure magnesite EOS [17] K_0 and K_0' and with the a_0 and c_0 found for the Fe–magnesite (color online).

In terms of Fe–Fe coordination, perovskite is closer to siderite, and indeed shows an increase in the transition pressure with dilution [22], however in the silicate, the lower symmetry and the mixed-valence isomorphous substitutions further complicate the scenario.

4. Conclusion

Fe dilution in the solid solution between siderite ($FeCO_3$) and magnesite ($MgCO_3$) induces a shift of the spin pairing transition to higher pressure. This behavior is consistent with a cooperative effect among adjacent clusters, the smaller the Fe concentration, the smaller the number of Fe–Fe

interactions, whether controlled by bonding or lattice strain. We note that in the periclase–wüstite solid solution the effect of Fe-dilution is opposite [19], possibly because the Fe–Fe repulsion and the strain induced by the smaller Mg atoms play a significant role.

Acknowledgements

The UNLV High Pressure Science and Engineering Center is supported by DOE-NNSA Cooperative Agreement DE-FC52-06NA262740. Diffraction data were collected at HPCAT (Sector 16), APS, Argonne National Laboratory. HPCAT is supported by CIW, CDAC, UNLV and LLNL through funding from DOE-NNSA, DOE-BES and NSF. APS is supported by DOE-BES, under Contract No. DE-AC02-06CH11357. We thank GSECARS and COMPRES for the use of the Gas Loading System. HPSynC is supported as part of the Efree, an Energy Frontier Research Center funded by DOE-BES under Award DE-SC0001057.

References

[1] M. Isshiki, T. Irifune, K. Hirose, S. Ono, Y. Ohishi, T. Watanuki, E. Nishibori, M. Takata, and M. Sakata, *Stability of magnesite and its high-pressure form in the lowermost mantle*, Nature 427 (2004), pp. 60–63.
[2] C. Biellmann, P. Gillet, F. Guyot, J. Peyronneau, and B. Reynard, *Experimental-evidence for carbonate stabiity in the Earth's lower mantle*, Earth Planet. Sci. Lett. 118 (1993), pp. 31–41.
[3] Y. Seto, D. Hamane, T. Nagai, and K. Fujino, *Fate of carbonates within oceanic plates subducted to the lower mantle, and a possible mechanism of diamond formation*, Phys. Chem. Miner. 35 (2008), pp. 223–229.
[4] F.E. Brenker, C. Vollmer, L. Vincze, B. Vekemans, A. Szymanski, K. Janssens, I. Szaloki, L. Nasdala, W. Joswig, and F. Kaminsky, *Carbonates from the lower part of transition zone or even the lower mantle*, Earth Planet. Sci. Lett. 260 (2007), pp. 1–9.
[5] A. Mattila, T. Pylkkanen, J.-P. Rueff, S. Huotari, G. Vanko, M. Hanfland, M. Lehtinen, and K. Hamalainen, *Pressure induced magnetic transition in siderite $FeCO_3$ studied by X-ray emission spectroscopy*, J. Phys: Condens. Matter 19 (2007), 386206.
[6] H. Shi, W. Luo, B. Johansson, and R. Ahuja, *First-principles calculations of the electronic structure and pressure-induced magnetic transition in siderite $FeCO_3$*, Phys. Rev. B 78 (2008), pp. 155119-1–7.
[7] B. Lavina, P. Dera, R.T. Downs, V. Prakapenka, M. Rivers, S. Sutton, and M. Nicol, *Siderite at lower mantle conditions and the effects of the pressure-induced spin-pairing transition*, Geophys. Res. Lett. 36 (2009), L23306.
[8] W. Fyfe, *The possibility of* d*-electron coupling in olivine at high pressures*, Geochim. Cosmochim. Acta 19 (1960), pp. 141–143.
[9] J. Badro, G. Fiquet, F. Guyot, J. Rueff, V. Struzhkin, G. Vanko, and G. Monaco, *Iron partitioning in Earth's mantle: Toward a deep lower mantle discontinuity*, Science 300 (2003), pp. 789–791.
[10] J.-F. Lin, G. Vanko, S.D. Jacobsen, V. Iota, V.V. Struzhkin, V.B. Prakapenka, A. Kuznetsov, and C.-S. Yoo, *Spin transition zone in Earth's lower mantle*, Science 317 (2007), pp. 1740–1743.
[11] J.-F. Lin, H. Watson, G. Vanko, E.E. Alp, V.B. Prakapenka, P. Dera, V.V. Struzhkin, A. Kubo, J. Zhao, C. McCammon, W.J. Evans, *Intermediate-spin ferrous iron in lowermost mantle post-perovskite and perovskite*, Nature Geosci. 1 (2008), pp. 688–691.
[12] J. Li, V. Struzhkin, H. Mao, J. Shu, R. Hemley, Y. Fei, B. Mysen, P. Dera, V. Prakapenka, and G. Shen, *Electronic spin state of iron in lower mantle perovskite*, Proc. Nat. Acad. Sci. USA 101 (2004), pp. 14027–14030.
[13] A. Hammersley, S. Svensson, A. Thompson, H. Graafsma, A. Kvick, and J. Moy, *Calibration and correction of distortions in 2-dimensional detector systems*, Rev. Sci. Instrum. 66 (1995), pp. 2729–2733.
[14] P. Dera, B. Lavina, L.A. Borkowski, V.B. Prakapenka, S.R. Sutton, M.L. Rivers, R.T. Downs, N.Z. Boctor, and C.T. Prewitt, *High-pressure polymorphism of Fe_2P and its implications for meteorites and Earth's core*, Geophys. Res. Lett. 35 (2008), L10301.
[15] Y. Fei, A. Ricolleau, M. Frank, K. Mibe, G. Shen, and V. Prakapenka, *Toward an internally consistent pressure scale*, Proc. Natl. Acad. Sci. USA 104 (2007), pp. 9182–9186.
[16] R.J. Angel, *Equations of State*, High-pressure and High-temperature Crystal Chemistry, Mineralogical Society of America and the Geochemical Society, Washington, DC, 2000, pp. 35–60.
[17] K.D. Litasov, Y. Fei, E. Ohtani, T. Kuribayashi, and K. Funakoshi, *Thermal equation of state of magnesite to 32 GPa and 2073 K*, Phys. Earth Planet. Inter. 168 (2008), pp. 191–203.
[18] J. Zhang, I. Martinez, F. Guyot, and R. Reeder, *Effects of Mg–Fe^{2+} substitution in calcite-structure carbonates: Thermoelastic properties*, Am. Mineral. 83 (1998), pp. 280–287.
[19] Y. Fei, L. Zhang, A. Corgne, H. Watson, A. Ricolleau, Y. Meng, and V. Prakapenka, *Thermal equation of state of magnesite to 32 GPa and 2073 K*, Geophys. Res. Lett. 34 (2007), L17307.
[20] M. Boiocchi, F. Caucia, M. Merli, D. Prella, and L. Ungaretti, *Crystal-chemical reasons for the immiscibility of periclase and wüstite under lithospheric P, T conditions*, Eur. J. Miner. 13 (2001), pp. 871–881.
[21] C. McCammon and L. Liu, *The effects of pressure and temperature on nonstoichiometric wüstite, Fe_xO-the iron-rich phase-boundary*, Phys. Chem. Miner. 10 (1984), pp. 106–113.
[22] A. Bengtson, K. Persson and D. Morgan, Ab initio *study of the composition dependence of the pressure-induced spin crossover in perovskite (Mg_{1-x},Fe_x)SiO_3*, Earth. Planet. Sci. Lett. 285 (2008), pp. 535–545.